Complex Spatial/Temporal CFAR

Z. Ebrahimian
Communication Sciences Institute, Department of Electrical Engineering-Systems
University of Southern California, Los Angeles, California, 90089-2565
zebrahim@usc.edu

Abstract

The conventional cell averaging Constant False Alarm Rate (CFAR) criterion and its variations work well only in strictly spatially stationary environments. In non-homogeneous environments, clutter map (scan-by-scan) processing is deployed. The performance of this method degrades in the presence of slow targets. In this paper, a hybrid procedure for CFAR is proposed, which combines the advantages of both spatial and time averaging. The detection probability is derived and the related plots are given for different values of L, the number of persistence scans. A method is presented to choose the parameter of the hybrid CFAR to have the lowest self-masking effect.

I. Introduction

The returned signal in a radar receiver is composed of target reflections, signal reflection from clutter points, and thermal noise in the receiver input. With a constant threshold in a clutter environment, false alarm probability is extremely sensitive to variations in average power of the clutter signal. Although it is possible to decrease the false alarm rate by choosing a high threshold, this will decrease system sensitivity to the target in low clutter regions, and reduce detection probability. Accordingly a constant false alarm rate (CFAR) approach is used to adaptively select the detection threshold. In these types of detectors, in order to declare a target, one checks for presence of the target signal, in the cell under test, which is strong enough for the reference cells. Three important ways for determining the threshold in an adaptive manner are parametric CFAR, non-parametric CFAR, and Clutter-Map. In the two first cases, it is assumed that the samples in the adjacent cells to the test cell (which are known as reference cells and can be expanded in the range, azimuth, or doppler domain) are iid, and a function of those will be used as threshold. The main assumption in parametric CFAR is that the probability density of interference is known but its parameters are not identified. Reference window cells are then used to estimate the unknown parameters and the threshold is determined based on these. Fig. 1 shows a simple CA-CFAR (Cell Averaging) of this group. This method is predicated upon the presence of clutter with stationary statistics. As such, in the case of moving rainstorms, or jamming and interference with signals of other radars, the false alarm rate may rapidly increase. Also these methods show a considerable drop in quality in the clutter edge or in the case of multiple interfering targets. Clutter-MAP was produced to counter with non-homogenous clutter. In these methods, the signal level in the cell under test, over successive scans, is used to estimate the interference level instead of averaging on the adjacent cells. This method is not affected by non-homogenous backgrounds and increases sub-clutter visibility ([1], [2]). In non-homogenous environments, CM-CFAR (Clutter Map-CFAR) shows much better performance than CA-CFAR. In CM-CFAR, the assumption is that the clutter samples are independent over scan by scan.

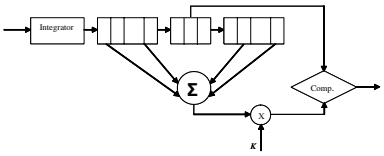

Fig. 1. CA-CFAR processor

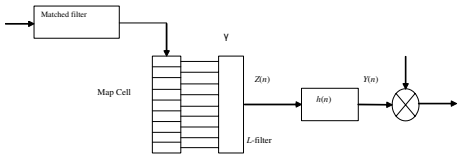

Fig. 2. CM/L-CFAR block diagram

In spite of the above mentioned advantages for methods based on clutter-map, their capabilities are limited by high amounts of memory requirement, transition response, and velocity response. Detection loss for slow targets is increased by velocity response limitation and thus causes the self-masking problem. To improve these drawbacks, complex methods of spatial and time-averaging CFAR are used. One of these complex procedures was proposed in [3](Fig. 2). In this method, sample cancellation by the Ll-Filter [4] before the clutter map is a very useful way to decrease self-masking and interfering target masking.
In this paper, we propose a new complex method of spatial and temporal CFAR (see Fig. 4). In this method some percentage of the detection threshold is obtained from CM-CFAR and the rest

This work was done while the author was a graduate student at the Isfahan University of Technology.

Report Documentation Page

Form Approved
OMB No. 0704-0188

1. REPORT DATE	2. REPORT TYPE	3. DATES COVERED
01 JAN 2005	**N/A**	**-**

4. TITLE AND SUBTITLE	5a. CONTRACT NUMBER
Complex Spatial/Temporal CFAR	5b. GRANT NUMBER
	5c. PROGRAM ELEMENT NUMBER
6. AUTHOR(S)	5d. PROJECT NUMBER
	5e. TASK NUMBER
	5f. WORK UNIT NUMBER
7. PERFORMING ORGANIZATION NAME(S) AND ADDRESS(ES) **Communication Sciences Institute, Department of Electrical Engineering-Systems University of Southern California, Los Angeles, California, 90089-2565**	8. PERFORMING ORGANIZATION REPORT NUMBER
9. SPONSORING/MONITORING AGENCY NAME(S) AND ADDRESS(ES)	10. SPONSOR/MONITOR'S ACRONYM(S)
	11. SPONSOR/MONITOR'S REPORT NUMBER(S)

12. DISTRIBUTION/AVAILABILITY STATEMENT
Approved for public release, distribution unlimited

13. SUPPLEMENTARY NOTES
See also ADM001846, Applied Computational Electromagnetics Society 2005 Journal, Newsletter, and Conference., The original document contains color images.

14. ABSTRACT

15. SUBJECT TERMS

16. SECURITY CLASSIFICATION OF:			17. LIMITATION OF ABSTRACT	18. NUMBER OF PAGES	19a. NAME OF RESPONSIBLE PERSON
a. REPORT	b. ABSTRACT	c. THIS PAGE			
unclassified	**unclassified**	**unclassified**	**UU**	**5**	

from temporal CFAR (thus $\alpha + \beta = 1$). This preserves the CM-CFAR immunity against spatial non-homogeneities and simultaneously exploits the good velocity response of spatial CFAR.
The rest of the paper is organized as follows. First the theoretical analysis of the new method is given. Then, the self-masking effect on the system performance is investigated. The experimental results is described at the end.

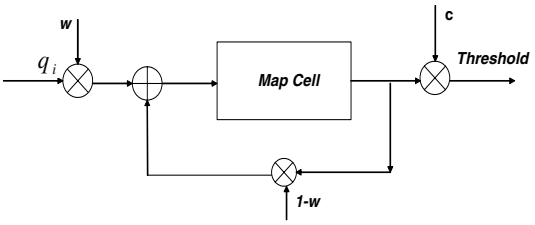

Fig. 3. CM-CFAR block diagram

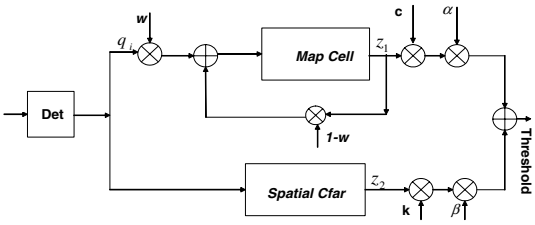

Fig. 4. Complex S/T CFAR

II. Spatial/Temporal CFAR

The proposed method was shown in Fig. 4. The mathematical analysis is given in below.

A. Analysis

Theoretical analysis of the proposed new method, when CA-CFAR is used in the spatial averaging branch, is presented here. Assuming a square-law detector, Gaussian noise and Swerling II model for target, the relations between false alarm probability and detection probability in optimum case are [5]

$$P_{fa} = P[y > y_0|H_0] = \int_{y_0}^{\infty} 1/2\mu * exp(-x/2\mu)dx = exp(-y_0/2\mu) \tag{1}$$

$$P_d = P[y > y_0|H_1] = \int_{y_0}^{\infty} 1/2\mu(1+S) * exp(-x/2\mu(1+S))dx = exp(-y_0/2\mu(1+S)), \tag{2}$$

where y_0 is threshold, μ is noise power for each cell, and S is target signal to noise power ratio. H_1 and H_0 represent hypotheses relating to the presence or absence of target respectively. In the CFAR processor, these probabilities are computed on a window, and are then averaged on the probability density of Z, the random variable of reference samples over all windows. In the complex method presented here, Z is composed of two random variables, z_1 and z_2, which are the samples that participate in spatial and temporal CFAR respectively. Therefore the detection and false alarm probability functions are

$$\begin{aligned} P_{fa} &= E_{z_1,z_2}\{P[y > (\alpha c z_1 + \beta k z_2)|H_0]\} \\ &= E_{z_1,z_2}\{\textstyle\int_{\alpha c z_1 + \beta k z_2}^{\infty} 1/2\mu exp(-y/2\mu)dy\} \\ &= E_{z_1,z_2}\{exp(-(\alpha c z_1 + \beta k z_2)/2\mu). \end{aligned} \tag{3}$$

Assuming a Swerling II model for the target, all samples are independent. Therefore

$$\begin{aligned} P_{fa} &= E_{z_1}\{exp\tfrac{-(\alpha c z_1)}{2*\mu}\} * E_{z_2}\{exp\tfrac{-(\beta k z_2)}{2\mu}\} \\ &= M_{z_1}\{\tfrac{\alpha c}{2\mu}\} * M_{z_2}\{\tfrac{\beta k}{2\mu}\}. \end{aligned} \tag{4}$$

Similarly, the detection probability is given by

$$\begin{aligned} P_d &= E_{z_1,z_2}\{P[y > (\alpha c z_1 + \beta k z_2)|H_1]\} \\ &= M_{z_1}\{\tfrac{\alpha c}{2\mu(1+S)}\} * M_{z_2}\{\tfrac{\beta k}{2\mu(1+S)}\}. \end{aligned} \tag{5}$$

Applying the equations given in [5], [6], for the CA-CFAR processor

$$M_{z_1}(u) = (1 + 2\mu\frac{u}{N})^{-N}, \tag{6}$$

where N is the number of cells that are used in the estimation. For CM-CFAR

$$M_{z_2}(u) = \prod_{l=0}^{\infty}[1 + 2\mu uw(1-w)^l]^{-1}. \tag{7}$$

The equations for false alarm and detection probability are thus obtained as

$$P_{fa} = \{\prod_{l=0}^{\infty}[1 + \alpha cw(1-w)^l]^{-1}\} * (1 + \frac{\beta k}{N})^{-N} \tag{8}$$

$$P_d = \{\prod_{l=0}^{\infty}[1 + \frac{\alpha cw}{1+S}(1-w)^l]^{-1}\} * (1 + \frac{\beta k}{N(1+S)})^{-N}. \tag{9}$$

In the rest of this discussion samples of 1,000 scans will be considered. To compare the complex method with CA-CFAR and simple CM-CFAR, the parameters of the two methods were determined separately. For this purpose, with $P_{fa} = 1e-8$ and $N = 15$, the following were obtained (c is obtained via numeric calculation)

$$\begin{aligned} k &= 36.2182 \\ c &= 31.5945 \\ w &= 0.125. \end{aligned} \tag{10}$$

Note that the effective number of integrated pulses in CM-CFAR is $N_f = \frac{2-w}{w}$ [7]. Therefore, w was chosen in such a way that both branches in the complex CFAR (i.e., CM-CFAR and CA-CFAR) have the same integration window length.
In the next step, α and β were chosen as $\alpha = 0.4$ and $\beta = 0.6$, and false alarm and detection probabilities were computed by Eqs. (8) and (9). In this way, it can be observed that the false alarm probability decreases dramatically and reaches 1.1708e-10, a reduction by a factor of 85.41. Fig. 5 shows the curve of false alarm probability versus α for the above mentioned parameters. As observed, the false alarm rate has its minimum value in $\alpha = 0.52$ where it reaches 1/106.6 its primary value. Detection probability curves for three methods, CA-CFAR, CM-CFAR and complex CFAR are shown in Fig. 6. It is observed that the detection probability curve for complex CFAR is located between two other curves, therefore the detection loss of complex CFAR is less than CM-CFAR.

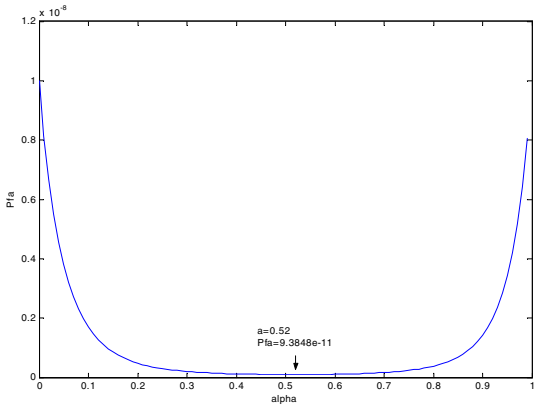

Fig. 5. P_{fa} versus α for complex S/T CFAR

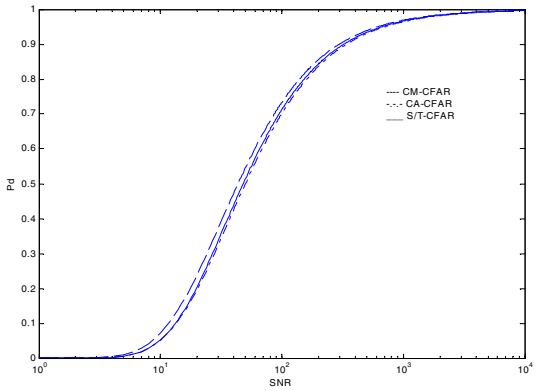

Fig. 6. Detection probability for three methods in homogenous environment

B. Self-Masking

In general, the density function of a LTI filter cannot be determined. But in the clutter-map filter shown in Fig. 3, the central limit theorem can apply when w goes to 0, because in this case, the integration modifies to averaging of an infinite number of random variables. Therefore, the output density function, regardless of the input density function, has a Gaussian distribution. The mean and variance of the filter output, as shown in [7] can be written based on input sequence x(i) as

$$Z(n-1) = w\sum_{i=0}^{n-1}(1-w)^{n-1-i}x(i). \tag{11}$$

Therefore the mean and variance of $Z(n)$ will be

$$\mu_z(n-1) = w\frac{1-b^n}{1-b}\mu_x \quad b \equiv (1-w) \tag{12}$$

$$\sigma_z^2(n-1) = w^2\frac{1-b^{2n}}{1-b^2}\sigma_x^2. \tag{13}$$

In the above equations, σ_x and μ_x are input sequence statistics of filter. When $n \longrightarrow \infty$, the steady state values of mean and variance will be

$$\mu_z(n-1) \longrightarrow \mu_z = \mu_x \tag{14}$$

$$\sigma_z^2(n-1) \longrightarrow \sigma_z^2 = \sigma_x^2/N_f \quad N_f = \frac{2-w}{w}. \tag{15}$$

To illustrate the system performance in presence of a slow target, it is assumed that the target enters the map cell in the nth scan and stays there for several scans. Therefore the filter output depends on two factors, Background estimation in steady state, and the number L of scans in which target stays in the same cell. As mentioned in [7], in this case, Eq. 11 modifies to

$$Z(n+L-1) = w\sum_{i=0}^{n-1} b^{n+L-1-i}n(i) + w\sum_{i=n}^{n+L-1} b^{n+L-1-i}x(i), \tag{16}$$

where n(i) is interference signal to the filter input before that target enters into the cell. The system has been assumed to be in steady state condition before the target enters the cell. Thus, the statistics of the filter output can be written as

$$\mu_z(n+L-1) \cong \mu_n * b^L + \mu_x * (1-b^L) \tag{17}$$

$$\sigma_z^2(n+L-1) \cong \frac{\sigma_n^2}{N_f}b^{2L} + \frac{\sigma_x^2}{N_f}(1-b^{2L}). \tag{18}$$

In the rest of discussion, the mean of interference and target will be considered as zero. In [7], to study system behavior in the presence of a self-masking target, it was assumed that the density function of the threshold is still Gaussian. Therefore

$$T(n+L-1) \propto N(\mu, \sigma), \tag{19}$$

with this assumption, the variance of the interference after the target entered into map cell, in the Lth scan in the input, can be written as [7]

$$\sigma_{n'}^2(n+L-1) \cong \frac{\sigma_n^2}{N_f}b^{2L} + \frac{\sigma_x^2}{N_f}(1-b^{2L}). \tag{20}$$

Signal-to-noise ratio for the scans in which the target has been in map cell is

$$S' = \frac{\sigma_x^2}{\sigma_{n'}^2}. \tag{21}$$

Replacing this value into Eq. (9), for the scans in which target is present in the map cell, gives the system performance for a slow target

$$P_d = \{\prod_{l=0}^{L-1}[1 + \frac{\alpha cw}{1+S_l'}(1-w)^l]^{-1}\prod_{l=L}^{\infty}[1 + \frac{\alpha cw}{1+S}(1-w)^l]^{-1}\}(1 + \frac{\beta k}{N(1+S)})^{-N} \tag{22}$$

where

$$\begin{array}{c} S_l' = \frac{\sigma_x^2}{\sigma_{n_l'}^2} \\ \sigma_{n_l'}^2 \cong \frac{\sigma_n^2}{N_f}b^{2l} + \frac{\sigma_x^2}{N_f}(1-b^{2l}) \end{array}. \tag{23}$$

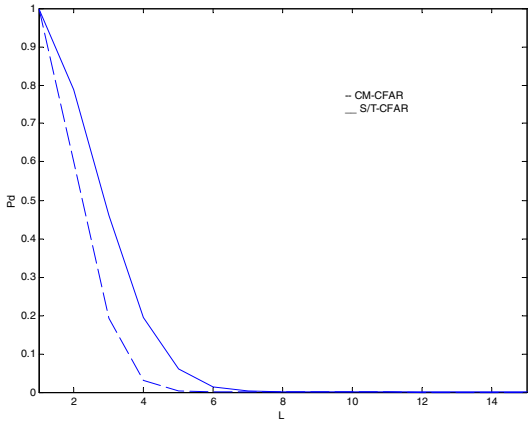

Fig. 7. Detection performance for a self-masking target for SNR=40dB, $\alpha = 0.4$

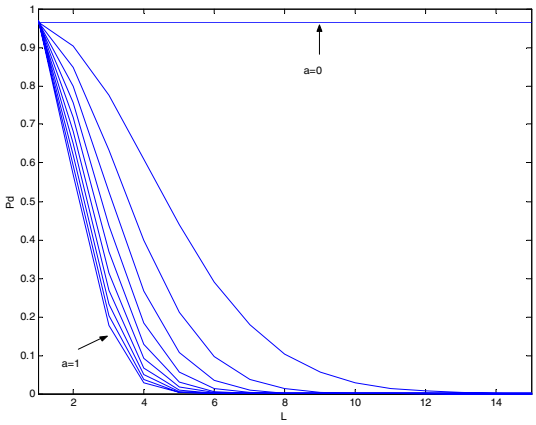

Fig. 8. Detection performance for a self-masking target for different value of α, SNR=40dB

Setting $\beta = 0$, the system performance while using just CM-CFAR is obtained. Detection probability curve for SNR=40dB is shown in Fig. 7. As is evident from this figure, the system performance for a slow target in complex CFAR is better than CM-CFAR.
Fig. 8 demonstrates the self-masking effect for different values of α ($0 \leq \alpha \leq 1$ with step 0.1). As expected, as CM-CFAR use increases in determining the threshold, so will the intensity of the self-masking effect. Considering Fig. 5 and 8, the parameter α can be determined. Since for a given P_{fa} two different values for α will be obtained, to decrease self-masking effect, smaller value has to be chosen.

III. Experimental Results

Practical observation of the proposed method showed that by using just CM-CFAR ($\alpha = 1, \beta = 0$), slow targets like helicopters are not observed. But in the combined method, this drawback has been diminished; furthermore , sub-clutter visibility has been increased. In this observation the detection performance of the proposed method was not less than CA-CFAR.

IV. Conclusions

In this paper, a combined method of spatial and temporal CFAR was introduced to benefit from their advantages at the same time. By using this method, three advantages are clearly evident: self-masking problem is decreased; sub-clutter visibility of CM-CFAR remains; and due to the sliding window in the spatial branch, periodic response is eliminated. While using spatial CFAR by itself sub-clutter visibility is extremely reduced; however, combining two methods gains both of their advantages simultaneously.

V. Acknowledgements

The author would like to thank Professors Hossein Alavi and Ali M. Doost Hosseini for valuable discussions, and everyone at the Information and Communication Technology Institute, Isfahan University of Technology.

References

[1] M.I Skolnik, *RADAR Handbook*, McGraw-Hill, 1990.
[2] J.S. Hoyle E.N Khoury, "Clutter maps: design and performance," *IEEE*, 1984.
[3] Peter Wilett Marco Lops, "Hybrid clutter-map/ l-cfar procedure for clutter rejection in nonhomogeneous environment," *IEE Proceedings*, vol. 143, no. 4, Aug 1996.
[4] Jr. Boncelet F. Palmieri; C.G., "Ll-filters-a new class of order statistic filters," *IEEE Transactions on Signal Processing*, vol. 37, no. 5, pp. 691 – 701, May 1989.
[5] S.A. Kassam P.P. Gandhi, "Analysis of cfar processors in homogeneous background," *IEEE Transactions on Aerospace and Electronic Systems*, vol. 24, no. 4, pp. 427 – 445, July 1988.
[6] Ramon Nitzberg, "Clutter map cfar analysis," *IEEE AES*, vol. 22, no. 4, pp. 419–421, July 1986.
[7] M. Lops; M. Orsini, "Scan-by-scan averaging cfar," *IEE Proceedings-Radar, Sonar and Navigation*, vol. 136, no. 6, pp. 249 – 254, Dec. 1989.